Peak Effect in Polycrystalline Vortex Matter

I. K. Dimitrov,[1] N. D. Daniilidis,[1] C. Elbaum,[1] J. W. Lynn,[2] and X. S. Ling[1,*]

[1]*Department of Physics, Brown University, Providence, Rhode Island 02912, USA*
[2]*NIST Center for Neutron Research, Gaithersburg, Maryland 20899, USA*

(Received 24 January 2007; published 23 July 2007)

We report a study of the peak-effect phase diagram of a strongly disordered type-II superconductor V-21 at. %Ti using ac magnetic susceptibility and small-angle neutron scattering (SANS). In this system, the peak effect appears only at fields higher than 3.4 T. The sample is characterized by strong atomic disorder. Vortex states with field-cooled thermal histories show that both deep in the mixed state, as well as close to the peak effect, there exist no long-range orientationally ordered vortex lattices. The SANS scattering radial widths reveal vortex states ordered in the sub-μm scale. We conjecture that the peak effect in this system is a remnant of the Bragg glass disordering transition, but occurs on submicron length scales due to the presence of strong atomic disorder on larger length scales.

DOI: 10.1103/PhysRevLett.99.047001 PACS numbers: 74.25.Qt, 61.12.Ex

Vortex phases in type-II superconductors are manifestations of a complex interplay among various underlying interactions. Intervortex repulsions tend to drive the vortices into forming an ideal crystalline lattice with long-range order (LRO) [1]. However, in real type-II superconductors, disorder-induced pinning deforms the Abrikosov vortices and prevents the emergence of LRO in the vortex state, as predicted on theoretical grounds [2]. In contrast to the theoretical predictions [2], neutron scattering experiments since the early 1970s [3,4] have provided strong evidence for the existence of an ordered phase in the mixed state of bulk niobium samples. In the 1990s, Nattermann [5] and Giamarchi and Le Doussal [6] revisited the random pinning problem and found that a *quasi*-ordered "Bragg glass" phase could exist in the mixed state of bulk type-II superconductors with weak random pinning. The existence of a topologically ordered phase at low temperatures implies the presence of a true symmetry-breaking phase transition. Indeed, a phase transition of the order-disorder type has been observed in a niobium crystal using small-angle neutron scattering (SANS) [7] and in a 2H-$NbSe_2$ crystal by real-space imaging using scanning tunneling microscopy [8].

Interestingly, the Bragg glass disordering transition was observed to coincide with the well-known anomaly of the peak effect in critical current [7,8]. The peak effect has been shown to be ubiquitous in many weakly disordered type-II superconductors, such as 2H-$NbSe_2$ [9], MgB_2 [10], and YBCO [11,12]. It has been interpreted previously using the standard model of "collective pinning" [13,14] as resulting from softening of the elastic moduli of the vortex lattice. In light of recent observations [7,8], the peak effect is now widely interpreted as evidence for a Bragg glass transition. However, it has been known that some strongly disordered bulk type-II superconductors, such as certain binary alloys (e.g., Nb-Ti, etc.) exhibit a peak effect as well [15,16]. There have been few prior experimental studies of the vortex structures in these systems and little is known about their vortex states.

Ideally, one would like to directly visualize the vortex structures in the peak-effect regime using STM [8] or Bitter decoration [17]. However, STM requires atomically flat sample surfaces and Bitter decoration can only access low magnetic fields. Here, we use neutron diffraction to probe the vortex-lattice structure in a strongly disordered binary alloy superconductor V-Ti, which exhibits a peak effect below its bulk superconducting transition at high fields. Measurements with field-cooled thermal histories both deep within the mixed state and close to the peak-effect regime show no signature of LRO in the vortex state. It is conjectured that the peak effect in this system corresponds to a disordering of locally ordered vortex lattices; it is the remnant of the Bragg glass disordering transition.

The sample is a binary alloy of nominal composition V-21 at. %Ti previously used in experiments by Shapira and Neuringer [15]. It is a parallelepiped with dimensions $7.4\,\text{mm} \times 7.4\,\text{mm} \times 11\,\text{mm}$, with a zero field $T_c = 7.3$ K, and a Ginzburg-Landau parameter $\kappa_1(0) \approx 26$ [18–20]. In the experiments by Shapira and Neuringer, the sample was annealed in vacuum [15]. After the annealing process, the change in the ultrasonic attenuation α versus field H at constant temperature ($T = 1.5$ K) was measured and an anomalous dip was observed to exist below the bulk superconducting transition [15]. This dip was identified with the occurrence of a peak effect in J_c [15].

In the present work, the atomic composition and order of the V-Ti sample are studied. The Laue backscattering pattern shows several sets of distinct diffraction peaks originating from a variety of atomic crystal lattice orientations [18]. This indicates the existence of single crystalline grains, at least tens of microns in size [21]. A scanning electron micrograph (SEM) of the heavily etched sample surface is shown in the inset of Fig. 1. Domains of a few hundred μm in size (identified as "phase A") are separated by an interconnected network ("phase B") which has been partially removed by the etchant. The width of phase B is on the order of a few micrometers and consequently phase B is estimated to comprise only 1%–2% of the sample

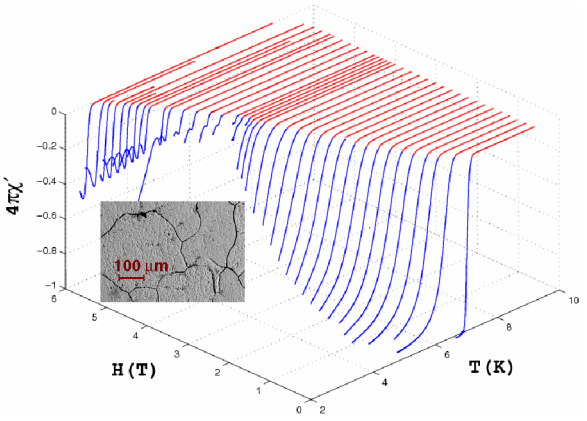

FIG. 1 (color online). Three-dimensional (3D) magnetic field and temperature dependence of the real part of the ac susceptibility $4\pi\chi'(T)$. Field-cooling scans, performed with $H_{ac} = 58$ Oe at $f = 107$ Hz. The color codes highlight the normal (red) and superconducting phases (blue). Inset: SEM image of a heavily etched sample surface. The visible domains (termed "phase A") contain approximately 20% titanium. The etched grooves surrounding phase A domains show the extent of a second phase (phase B), with elevated titanium content.

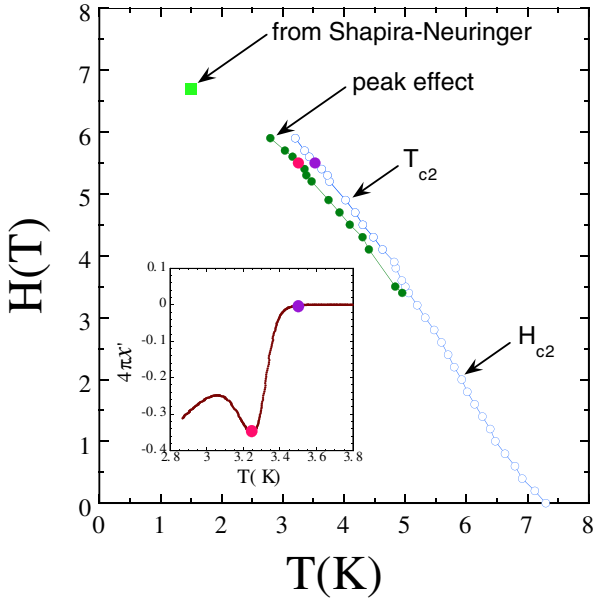

FIG. 2 (color online). Phase diagram constructed from the $4\pi\chi'(T)$ data (shown in Fig. 1). The filled green and empty blue circles correspond to the occurrences of the peak effect and the bulk superconducting transitions below and above the peak effect (H_{c2} and T_{c2}, respectively). H_{c2} and T_{c2} are defined to be at the temperature, at which $4\pi\chi' = -0.001$. The filled green square is extracted from the ultrasonic attenuation α vs H at $T = 1.5$ K scan of Shapira and Neuringer, performed on the same sample [15]. Inset: typical $4\pi\chi'(T)$ scan for fields at which the peak effect is readily visible ($H = 5.5$ T). The points marked in pink and violet are the locations of the peak effect and T_{c2} shown at $H = 5.5$ T in the phase diagram.

volume [18]. An energy-dispersive x-ray analysis indicates that in phase A the titanium contents fluctuate between 19%–21% [18] and that phase B is characterized by elevated titanium content (typically between 25%–67%) [18]. Upon electro-polishing the sample, etch pits form on the surface in the phase A domains and in certain regions they tend to line up, indicating the existence of edge dislocations and low-angle grain boundaries inside the phase A domains.

Inside the atomic crystallites, the vortex lattice will experience random point disorder. At larger scales the dislocations and grain boundaries will act as sources of correlated disorder. At the largest length scales (~ 100 μm) the varying atomic composition corresponding to phase A and phase B will also introduce strong correlated disorder. Based on its composition, phase B has both a higher transition temperature and upper critical field than phase A [18,22,23].

In order to map out the vortex matter phase diagram, the ac magnetic susceptibility was measured via a mutual-inductance technique with phase sensitive lock-in detection [11]. χ' is a measure of the critical current density, where a dip in χ' corresponds to a peak in J_c [11]. Figure 1 shows a three-dimensional plot of the evolution of $\chi'(T)$ in V-Ti as a function of temperature and magnetic field in the range of fields between 0–6 T in steps of 0.2 T.

A shoulderlike feature appears at an applied dc field of $H_\ell = 3.4$ T. It gradually transforms into a well-pronounced dip with increasing field, unlike the sudden appearance of a peak effect observed in single crystal niobium [24]. As shown in the phase diagram in Fig. 2, the peak effect vanishes at $H < H_\ell = 3.4$ T, and no reentrant behavior of the peak effect is observed at low fields.

The peak effect appears at H_ℓ, but only when probed with the highest H_{ac} used ($H_{ac} = 58$ Oe), while at lower H_{ac} it becomes resolved at higher H. This situation is similar to the one reported in niobium [24]. The main difference is that in niobium the peak effect appears at a field approximately $0.15H_{c2}(0)$, while here it appears at a considerably higher field, $0.47H_{c2}(0)$. What controls the location of H_ℓ ("critical point" in [24]) remains a major puzzle concerning the physics of the peak effect.

An important question for the V-Ti system is whether the vortex structure below the peak effect possesses LRO, and we address this using small-angle neutron scattering (SANS) [3,4,7]. We performed SANS measurements on the 30 m SANS instrument NG-3 at the NIST Center for Neutron Research. The incident neutron beam had a mean wavelength of $\lambda_n = 6.0$ Å and wavelength spread of 14% (FWHM). A cadmium mask shielded the edges of the sample, exposing only its central region to the neutron flux. The angle ϕ between the direction of the incoming neutrons and the applied horizontal field H was changed in 0.25° increments and subsequently, measurements at fixed H, T, and ϕ were taken. All of the SANS measurements were performed after in-field cooling (FC). The measured reciprocal lattice constants are consistent with the theoretically predicted values for hexagonal Abrikosov vortex

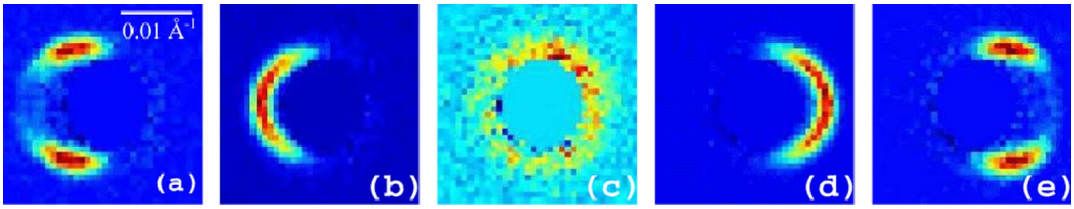

FIG. 3 (color online). (a)–(e) SANS images taken on FC deep in the mixed state of V-Ti, at $T = 4.2$ K, $H = 0.4$ T, and turning angle (a) $\phi = 0.50°$, (b) $\phi = 0.25°$, (c) $\phi = 0.00°$, (d) $\phi = -0.25°$, and (e) $\phi = -0.50°$. The intensity maximum occurs at $Q_r = 0.009\,173 \pm 0.000\,192$ Å^{-1}, whereas the expected value for a hexagonal Abrikosov lattice is $Q_r = 0.009\,386$ Å^{-1} [18].

lattices showing that the diffraction peaks indeed come from vortex structures [18].

In Fig. 3 we show the evolution of the SANS diffraction pattern from a field-cooled vortex state at $T = 4.2$ K and $H = 0.4$ T at a variety of angles ϕ. The evolution of the patterns shows well-defined intensity maxima at the largest angles shown ($\phi = \pm 0.50°$). These maxima commence to fuse as the rocking angle is changed to $\phi = \pm 0.25°$, forming a single intensity sliver. Finally, when the orientation of the incoming neutron beam is aligned with H at $\phi = 0°$, the resulting neutron diffraction pattern is a nearly uniform diffraction ring, which would be expected for an orientationally disordered structure.

The patterns in Fig. 3 are best explained by using the Ewald construction [25] method. The Ewald sphere radius (k) is determined by λ_n ($k = 2\pi/\lambda_n \approx 1.05$ Å^{-1}) and the Bragg condition is met whenever the surface of the Ewald sphere intersects the reciprocal lattice structure. The reciprocal lattice of an orientationally disordered vortex structure is a set of concentric rings of finite width and thickness, with radii nQ_r, where n is an integer and Q_r is determined by the vortex density ($Q_r \approx \sqrt{B/\Phi_0}$, Φ_0 being the flux quantum). Rotating the sample is equivalent to rotating the reciprocal lattice with respect to the Ewald sphere. Constructive interference occurs at the resulting intersections of the Ewald sphere with a three-dimensional torus in q space, and our calculations based on the above premise produce the correct angular dependence of the separation between the maxima observed in Fig. 3(a) and 3(e).

We performed neutron diffraction measurements close to the peak-effect region and the results are shown in Fig. 4. The Ewald-construction analysis suggests that these results are consistent with the scattering from an orientationally disordered lattice. On further approaching the peak-effect region, for example, at 3.7 T and temperatures higher than 3.6 K, no diffraction features from the vortex lattice can be discerned beyond scattering from the background, due to the long penetration depth of the system. From the data presented in Figs. 3 and 4, we conclude that the vortex states in V-Ti, both deep in the mixed state and in the neighborhood of the peak effect, do not exhibit the signatures of orientational LRO.

The question then arises as to whether the vortex matter system possesses short-range order from which the remnant of the Bragg glass transition could lead to a peak effect. Our data do indeed indicate an increase in the level of local order as the field is increased from 0.4 T to 3.7 T. Radial averages of normalized intensity versus q are shown in Fig. 4(c). At low field, 0.4 T, the FWHM radial spread is larger than the instrumental resolution and approximately given by 2.4×10^{-3} Å^{-1}. At 3.7 T, the radial width 3.4×10^{-3} Å^{-1} which is the resolution limit. These values imply that the vortex structure is ordered in the transverse direction on the scale of 0.07 μm at 0.4 T and on a scale significantly larger than 0.05 μm at 3.7 T. These lengths correspond to 6 and 13 vortex-lattice spacings, respectively.

We can compare these results with estimates of the Larkin-Ovchinnikov domain size in the context of the collective-pinning model [14]. We use the χ' results of Fig. 1 to estimate critical current densities [11]. We estimate the critical current density at 4.2 K, 0.4 T to be 300 A/cm^2 and at 3.6 K, 3.7 T to be approximately

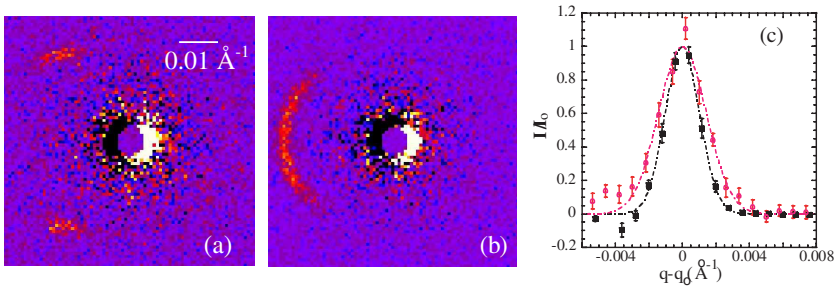

FIG. 4 (color online). (a)–(b) SANS images taken closer to the peak-effect regime, at $H = 3.7$ T, $T = 3.6$ K. (a) $\phi = 0.25°$ and (b) $\phi = 0.75°$. (c) Radial averages of the scattered intensity at 0.4 T (black, squares) and 3.7 T (red, circles). At high field the radial width is resolution limited, implying higher degree of translational order at high field.

200 A/cm^2. The transverse dimensions of the Larkin domains are on the order of 6 μm and 2 μm, respectively. The former is larger than the experimentally determined value of 0.07 μm by a factor of 100. Thus the collective-pinning model does not apply to the strongly disordered sample in our studies. This comes as no surprise, since the existence of grain boundaries and strong modulation in the atomic composition will very likely induce plastic vortex-lattice deformations. For this reason the phenomenological treatments [26] of the peak-effect phase diagrams are inapplicable to this V-Ti sample.

We argue that, in spite of the lack of a bulk Bragg glass with LRO, the peak effect in this sample may still be caused by a disordering process. It is conceivable that the vortex structure is locally ordered inside the crystallites of the atomic lattice. This gives rise to a polycrystalline vortex lattice, or more correctly, a poly-Bragg glass, as reported previously [17] in 2H-$NbSe_2$. In this case, the disordering within the microcrystalline domains gives rise to the observed peak effect. Given that the underlying Bragg glass transition is first order [7], this conclusion may not be surprising according to the Imry-Wortis criterion [27].

In this context, it is interesting to recall that the peak effect disappears in this V-21 at. %Ti sample at fields much higher than in the niobium sample previously studied by some of us [7,24]. If the peak effect is a remnant of the Bragg glass transition, this can be related to a spatial confinement effect. In the study of first-order transitions, it is well known that spatial confinement can inhibit the occurrence of the transition. This happens because nuclei of the ordered phase are unstable below some critical size R_c: the surface energy cost $\sim R^2$ dominates over the bulk energy gain $\sim R^3$ at small nucleus sizes R [28]. In our case, the Bragg glass transition is confined to occur inside the atomic crystal grains. However, for a given atomic crystallite size, the size of a vortex crystallite in units of vortex-lattice spacings grows as $B^{1/2}$ with increasing field. At field $H_\ell \approx 3.4$ T the critical size for nucleation of stable Bragg glass crystallites drops below the typical atomic grain size, giving rise to the gradual appearance of the peak effect.

In conclusion, we have mapped out the peak-effect phase diagram in V-21 at. %Ti. Our SANS measurements show that the vortex states below the peak effect do not possess LRO. The SANS radial intensity profile shows short-range order at length scale larger than 13 lattice constants at $H = 3.7$ T. The peak effect is proposed to be the disordering of this polycrystalline vortex lattice and constitutes the remnant of the Bragg glass disordering transition. The absence of the peak effect until relatively high fields is attributed to a confinement effect on first-order phase transitions.

We thank Professor Y. Shapira of Tufts University for providing the sample and D. Dender and B. Greenwald of NCNR-NIST for technical assistance. This work was supported by the NSF under Grant No. NSF-DMR-04046626 and used facilities supported in part by the NSF under Grant No. NSF-DMR-0454672.

*Corresponding author.
xsling@brown.edu

[1] A. A. Abrikosov, Sov. Phys. JETP **5**, 1174 (1957).
[2] A. I. Larkin, Sov. Phys. JETP **31**, 784 (1970).
[3] J. Schelten, H. Ullmaier, and W. Schmatz, Phys. Status Solidi B **48**, 619 (1971).
[4] D. K. Christen, F. Tasset, S. Spooner, and H. A. Mook, Phys. Rev. B **15**, 4506 (1977).
[5] T. Nattermann, Phys. Rev. Lett. **64**, 2454 (1990).
[6] T. Giamarchi and P. Le Doussal, Phys. Rev. Lett. **72**, 1530 (1994); Phys. Rev. B **52**, 1242 (1995).
[7] X. S. Ling, S. R. Park, B. A. McClain, S. M. Choi, D. C. Dender, and J. W. Lynn, Phys. Rev. Lett. **86**, 712 (2001).
[8] A. M. Troyanovski, M. van Hecke, N. Saha, J. Aarts, and P. H. Kes, Phys. Rev. Lett. **89**, 147006 (2002).
[9] S. Bhattacharya and M. J. Higgins, Phys. Rev. Lett. **70**, 2617 (1993).
[10] M. Pissas, S. Lee, A. Yamamoto, and S. Tajima, Phys. Rev. Lett. **89**, 097002 (2002).
[11] X. S. Ling and J. I. Budnick, in *Magnetic Susceptibility of Superconductors and Other Spin Systems*, edited by R. A. Hein *et al.* (Plenum, New York, 1991), p. 377.
[12] W. K. Kwok, J. A. Fendrich, C. J. van der Beek, and G. W. Crabtree, Phys. Rev. Lett. **73**, 2614 (1994).
[13] A. B. Pippard, Philos. Mag. **19**, 217 (1969).
[14] A. I. Larkin and Yu. N. Ovchinnikov, J. Low Temp. Phys. **34**, 409 (1979).
[15] Y. Shapira and L. J. Neuringer, Phys. Rev. **154**, 375 (1967).
[16] F. P. Missell, N. F. Oliveira, Jr., and Y. Shapira, Phys. Rev. B **14**, 2255 (1976).
[17] Y. Fasano, M. Menghini, F. de la Cruz, Y. Paltiel, Y. Myasoedov, E. Zeldov, M. J. Higgins, and S. Bhattacharya, Phys. Rev. B **66**, 020512(R) (2002).
[18] I. K. Dimitrov, Ph.D. thesis, Brown University, 2007.
[19] L. P. Gorkov, Sov. Phys. JETP **37**, 593 (1960).
[20] T. G. Berlincourt and R. R. Hake, Phys. Rev. **131**, 140 (1963).
[21] B. D. Cullity, *Elements of X-Ray Diffraction* (Addison-Wesley, Reading, MA, 1958).
[22] E. W. Collings, *A Sourcebook of Titanium Alloy Superconductivity* (Plenum, New York, 1983).
[23] Phase B does not cause any measurable diamagnetic signal in χ' above the average critical field (H_{c2} or T_{c2}) due to its very small volume fraction.
[24] S. R. Park, S. M. Choi, D. C. Dender, J. W. Lynn, and X. S. Ling, Phys. Rev. Lett. **91**, 167003 (2003).
[25] N. W. Ashcroft and N. D. Mermin, *Solid State Physics* (Saunders College Publishing, Philadelphia, 1976).
[26] G. Mikitik and E. H. Brandt, Phys. Rev. B **64**, 184514 (2001).
[27] Y. Imry and M. Wortis, Phys. Rev. B **19**, 3580 (1979).
[28] K. Binder, Rep. Prog. Phys. **50**, 783 (1987).